Photos: DOI: 10.1051/ogst/2013204, IFPEN, X.

Dossier

This paper is a part of the hereunder thematic dossier published in OGST Journal, Vol. 69, No. 4, pp. 507-766 and available online here

Cet article fait partie du dossier thématique ci-dessous publié dans la revue OGST, Vol. 69, n°4 pp. 507-766 et téléchargeable ici

DOSSIER Edited by/Sous la direction de : **Z. Benjelloun-Touimi**

Geosciences Numerical Methods
Modélisation numérique en géosciences

Oil & Gas Science and Technology – Rev. IFP Energies nouvelles, Vol. 69 (2014), No. 4, pp. 507-766

IFP Energies nouvelles

Oil & Gas Science and Technology – Rev. IFP Energies nouvelles, Vol. 69 (2014), No. 4, pp. 687-699

DOI: 10.2516/ogst/2013176

Dossier

Geosciences Numerical Methods
Modélisation numérique en géosciences

Adaptive Mesh Refinement for a Finite Volume Method for Flow and Transport of Radionuclides in Heterogeneous Porous Media

Brahim Amaziane[1]*, Marc Bourgeois[2] and Mohamed El Fatini[3]

[1] *Université de Pau et des Pays de l'Adour, Laboratoire de Mathématiques et de leurs Applications, CNRS-UMR 5142, Av. de l'Université, 64000 Pau - France*
[2] *Institut de Radioprotection et de Sûreté Nucléaire, PRP-DGE/SEDRAN/BERIS, BP 17, 92262 Fontenay-aux-Roses - France*
[3] *Université Ibn Tofail, Faculté des Sciences, LIRNE, EIM, BP 133, Kénitra - Morocco*
e-mail: brahim.amaziane@univ-pau.fr - marc.bourgeois@irsn.fr - melfatini@gmail.com

* Corresponding author

Résumé — **Adaptation de maillage pour un schéma volumes finis pour la simulation d'écoulement et de transport de radionucléides en milieux poreux hétérogènes** — Cet article traite de l'adaptation dynamique de maillages pour la simulation numérique d'écoulements incompressibles et miscibles en milieux poreux. Le problème est modélisé par un système couplé entre une équation elliptique (pression-vitesse de Darcy) et une équation de diffusion-convection (concentration). Le système est discrétisé par une méthode volumes finis centrés sur les sommets. On utilise un schéma de Godunov pour approcher le terme de convection et une approximation élément fini P1 pour le terme de diffusion. Nous développons des estimateurs d'erreur *a posteriori* de type résiduel. Nous introduisons deux sortes d'indicateurs. Le premier est local en temps et en espace et constitue un outil efficace pour l'adaptation du maillage à chaque pas de temps. Le second est global en espace mais local en temps et peut être utilisé pour l'adaptation en temps. La méthode proposée a été intégrée en deux dimensions d'espace dans le logiciel MELODIE développé par l'Institut de Radioprotection et de Sûreté Nucléaire (IRSN). La méthodologie d'adaptation de maillage décrite dans cet article est utilisée pour simuler des exemples de relâchement et de migration de radionucléides dans un stockage géologique de déchets radioactifs. Des résultats numériques d'adaptation dynamique de maillages sont présentés et montrent l'efficacité et la robustesse de la méthode.

Abstract — ***Adaptive Mesh Refinement for a Finite Volume Method for Flow and Transport of Radionuclides in Heterogeneous Porous Media*** — *In this paper, we consider adaptive numerical simulation of miscible displacement problems in porous media, which are modeled by single phase flow equations. A vertex-centred finite volume method is employed to discretize the coupled system: the Darcy flow equation and the diffusion-convection concentration equation. The convection term is approximated with a Godunov scheme over the dual finite volume mesh, whereas the diffusion-dispersion term is discretized by piecewise linear conforming finite elements. We introduce two kinds of indicators, both of them of residual type. The first one is related to time discretization and is local with respect to the time discretization: thus, at each time, it provides an appropriate information for the choice of the next time step. The second is related to space discretization and is local with respect to both the time and space variable and the idea is that at each time it is an efficient tool for mesh adaptivity. An error estimation procedure*

evaluates where additional refinement is needed and grid generation procedures dynamically create or remove fine-grid patches as resolution requirements change. The method was implemented in the software MELODIE, developed by the French Institute for Radiological Protection and Nuclear Safety (IRSN, Institut de Radioprotection et de Sûreté Nucléaire*). The algorithm is then used to simulate the evolution of radionuclide migration from the waste packages through a heterogeneous disposal, demonstrating its capability to capture complex behavior of the resulting flow.*

INTRODUCTION

Numerical modeling of flow and transport in porous media is significant for many petroleum and environmental engineering problems. Most recently, modeling multiphase flow has received increasing attention in connection with the disposal of radioactive waste and for CO_2 storage sequestration in geological formations.

The long-term safety of the disposal of nuclear waste is an important issue in all countries with a significant nuclear program. One of the solutions envisaged for managing waste produced by nuclear industry is to dispose of the radioactive waste in deep geological formations chosen for their ability to delay and to attenuate possible releases of radionuclides in the biosphere. Repositories for the disposal of high-level and long-lived radioactive waste generally rely on a multi-barrier system to isolate the waste from the biosphere. The multi-barrier system typically comprises the natural geological barrier provided by the repository host rock and its surroundings and an engineered barrier system, *i.e.* engineered materials placed within a repository, including the waste form, waste canisters, buffer materials, backfill and seals, for more details see for instance [1]. An important task of the safety assessment process is the handling of heterogeneities of the geological formation.

In this paper, we focus our attention on the numerical simulations of a single phase flow of an incompressible fluid with a dissolved radioactive solute: miscible flow, in connection with questions of safety of a nuclear waste repository. For more details on the formulation of such problems see, *e.g.*, [2, 3] and the references therein. Numerical simulation of flow and transport in porous media in petroleum and environmental applications has been a problem of interest for many years and many methods have been developed. There is an extensive literature on this subject. We will not attempt a literature review here, but merely mention a few references. We refer to the books [4-6] and the references therein.

In the safety assessment of deep geological repositories, a thoughtful consideration must be given to the mechanisms and possible pathways of migration of released radionuclides. However, when assessing confinement capabilities of disposal facilities and of the geological formations, the investigated domain covered by the numerical simulations includes a strong variability in the domain properties as well as in the geometrical scales (from cm to km) and presents significant computational challenges. Simulation models, if they are intended to provide realistic predictions, must accurately account for these effects. Furthermore, such flows are often characterized by localized phenomena such as steep concentration fronts. Accurately resolving these types of phenomena requires high resolution in regions where the solution is changing rapidly. For this reason, the development of some type of dynamic griding capability has long been of interest in the porous media community.

The adaptive mesh refinement has been a problem of interest for many years and many methods have been developed. There is an extensive literature on this subject for finite element approximations. Adaptive discontinuous Galerkin methods have tremendously developed in the last decade. We will not attempt a literature review here, but merely mention a few references. Here, we restrict ourself to adaptive methods for finite volume discretization in the context of flow and transport in porous media. Closely related to our work, we refer for instance to [7-25] and the references therein.

The French Institute for Radiological Protection and Nuclear Safety (IRSN) developed the code MELODIE, see for instance [26] and [27], and is constantly upgrading it, for numerical modeling of the physico-chemical phenomena involved in the release and in the migration of radionuclides from waste packages to the geosphere outlets (in deep geological formations, and more recently at surface or sub-surface locations). The mathematical formulation of these type of flow leads to a coupled system of partial differential equations, which includes an elliptic pressure-velocity equation and a diffusion-convection concentration equation. A vertex-centred finite volume method is employed to discretize the coupled system: the Darcy flow equation and the diffusion-convection concentration equation. The convection term is approximated with a Godunov scheme over the dual finite volume mesh, whereas the diffusion-dispersion term is discretized by piecewise linear conforming finite elements. The motivation for applying such finite volume procedure for modeling flow in porous media arises from the fact that this scheme is mass conservative element by

element and satisfies a discrete maximum principle. IRSN is constantly upgrading MELODIE to improve the resolution time, the accuracy and the confidence in the results of the simulations.

The purpose of this paper is to build *a posteriori* error estimators with a strategy of adaptive mesh refinement, implement the method in the code MELODIE and present numerical simulations. The estimators are expected to allow managing of the process of local refinement of the mesh in order to minimize the discretization error at an optimal computational cost. We introduce two kinds of indicators, both of them of residual type. The first one is related to time discretization and is local with respect to the time discretization: thus, at each time, it provides an appropriate information for the choice of the next time step. The second is related to space discretization and is local with respect to both the time and space variable and the idea is that at each time it is an efficient tool for mesh adaptivity. An error estimation procedure evaluates where additional refinement is needed and grid generation procedures dynamically create or remove fine-grid patches as resolution requirements change. The aim is to concentrate the computational work near the regions of interest in the flow, such as in regions where the solution is changing rapidly and around wells. This can significantly reduce the computational effort required to obtain a desired level of accuracy in the simulation.

The reminder of the paper is organized as follows. In the next section, we give a short description of the mathematical and physical model used in this study. The third section describes their discretization using a vertex-centred finite volume method and a semi-implicit Euler approach is used for time discretization. In the fourth section, we present the construction of the residual error estimators and the adaptive algorithm. Results from numerical simulations are presented in the fifth section. To validate the efficiency and the accuracy of the method, two tests are investigated for 2D miscible flow problems. In the first test, a domain made of two porous media separated by an interface with one source is considered. The second test addresses the evolution of radionuclide migration from the waste packages through a complex heterogeneous disposal made of six different layers, where large permeability variations are allowed, with three source terms. Finally, we give some conclusions and remarks on this work, and discuss some of our future research.

1 MODEL SYSTEM FOR MISCIBLE FLOW

We consider for simplicity a two-dimensional horizontal reservoir where the gravity effects are negligible. The single-phase flow of an incompressible fluid with a dissolved solute in a horizontal porous reservoir $\Omega \subset \mathbb{R}^2$ over a time period $]0, T_f[$, is given by Darcy's law and mass conservation (*e.g.*, [4-6]):

$$\vec{q} = -\frac{K(x)}{\mu(c)}\nabla P \text{ in } \Omega\times]0, T_f[\tag{1}$$

$$\operatorname{div}\vec{q} = 0 \text{ in } \Omega\times]0, T_f[\tag{2}$$

$$\omega(x)\frac{\partial C}{\partial t} - \operatorname{div}(D(x,\vec{q})\nabla C - C\vec{q}) = f \text{ in } \Omega\times]0, T_f[\tag{3}$$

where P and $\vec{q}$ are the pressure and Darcy velocity of the fluid mixture, ω and K are the porosity and the permeability of the medium, μ is the viscosity of the mixture, C is the concentration of the contaminant solute, and f is a given source term. D is the diffusion-dispersion tensor given by:

$$D(x,\vec{q}) = d_e I + |\vec{q}|[\alpha_l E(\vec{q}) + \alpha_t(I - E(\vec{q}))] \tag{4}$$

with $E_{ij}(\vec{q}) = \frac{q_i q_j}{|\vec{q}|^2}$, $1 \le i, j \le 2$, $|\vec{q}|$ is the Euclidean norm of $\vec{q}$, d_e is the effective diffusion coefficient, and α_l and α_t are the magnitudes of longitudinal and transverse dispersion respectively.

The system (1-3) is subjected to appropriate boundary conditions and an initial condition. In what follows we use standard assumptions for miscible flow in porous media. Namely, we will assume that the porosity ω is bounded above and below by positive constants, the permeability K and the diffusion-dispersion D are uniformly positive definite matrices, the viscosity μ is such that, $0 < \mu_- \le \mu(c) \le \mu^+$, $c \in [0, 1]$, and d_e, α_l and α_t are positive constants such that $\alpha_t \le \alpha_l$.

2 FINITE VOLUME DISCRETIZATION

For the spatial discretization of the system (1-3), we use the vertex-centered finite volume method, also called the control volume finite element method. We consider here the two dimensional case, for more details see for instance [2, 28] and the references therein. The method is based on two spatial grids: a primary grid, which is a conforming finite element grid, and a secondary grid composed of control volumes centered in the vertices of the primary grid. Control volumes are constructed around grid nodes by joining the midpoints of the edges of a triangle with the barycenter of the triangle (*Fig. 1*). All model data, permeability, porosity, sources, and dispersivity are constant element-wise on the primary grid. The material interfaces are therefore aligned with the

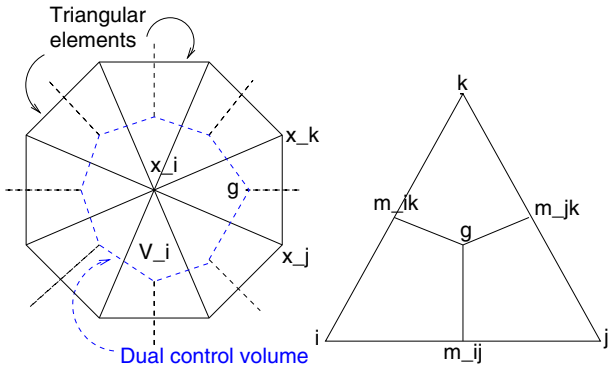

Figure 1

A vertex-centred cell and notations for the triangulation and the dual mesh.

edges of the primary grid. The pressure and concentration unknowns, are represented as P1 finite element functions over the primary grid.

Before introducing the scheme, let us give some definitions and notations for the meshes. We introduce a partition of the interval $[0, T_f]$ into sub-intervals $[t_{n-1}, t_n]$, $1 \leq n \leq N$ such that $0 = t_0 < t_1 < ... < t_N = T_f$. We denote by τ_n the length $t_{n+1} - t_n$, and by τ the maximum of τ_n, $1 \leq n \leq N$. For each n, we consider $\mathscr{T}_h^n$ a regular triangulation of Ω by closed triangles. We denote by $\mathscr{V}_h^n$ the dual decomposition associated to $\mathscr{T}_h^n$. The partition $\mathscr{V}_h^n$ is chosen as the set of $\mathscr{N}$ control volumes V_i that constitute the dual of the triangulation $\mathscr{T}_h^n$ known as the Voronoï mesh and such that $\overline{\Omega} = \cup_{i=1,...,\mathscr{N}} V_i$. The mesh is constructed by connecting the middle points of edges and circumcenters of each neighboring pair of triangles having a common edge with a straight-line segment. Furthermore, we denote by $\mathscr{E}_h^n$ the set of edges E of the triangulation $\mathscr{T}_h^n$, and Γ_h^n the set of edges γ of the dual decomposition $\mathscr{V}_h^n$. In the following, we denote respectively by σ_1 and σ_2 the edges gm_{ij} and gm_{ik} and by $\vec{n}_{\sigma_1}$ and $\vec{n}_{\sigma_2}$ their outward unit normals, and by Σ_1 et Σ_2 the sub-edges of T: im_{ij} and im_{ik}; and $\vec{n}_{\Sigma_1}$ and $\vec{n}_{\Sigma_2}$ their outward unit normals.

2.1 Discretization of the Flow Equation

To efficiently solve the governing equations, we use a sequential approach in which the pressure and concentration equations are solved consecutively. For simplicity, we will consider a permanent regime and take $\mu = 1$, so the time level is omitted to shorten the notation.

We now describe the space discretization with a vertex-centred finite volume scheme, (*e.g.*, [29]). Integrating Equation (2) over a control volume V_i and using the divergence theorem and (1), we get:

$$0 = -\int_{\partial V_i} K\nabla P.\vec{n}d\sigma \approx -\sum_{T;i\in T}\int_{\partial V_i\cap T} K_T\nabla P.\vec{n}d\sigma \quad (5)$$

where K_T is an approximation of the permeability tensor in T and i a vertex belonging to T. Denote by $\mathscr{V}_T(i) = \{j \text{ neighbor of } i\,; j \in T\}$, the neighbors of i belonging to T, and by:

$$a_{ij}^{flow}(T) = -\int_{\partial V_i\cap T} K_T\nabla N_j.\vec{n}d\sigma \quad (6)$$

the elementary diffusive term, where N_j is the P1 finite element base function on the triangle associated to the vertex x_j. Using a P1 Galerkin expansion of P and using the fact that $\sum_{j\in V_T(\mathrm{i})} N_j = 1$ in T, we obtain:

$$-\int_{\partial V_i} K\nabla P.\vec{n}d\sigma = \sum_{j\in V_T(\mathrm{i})} a_{ij}^{flow}(T)\left(P_j - P_i\right) = 0 \quad (7)$$

Observing that $\partial V_i \cap T = \sigma_1 \cup \sigma_2$, we get:

$$a_{ij}^{flow}(T) = -K_T\nabla N_j.(|\sigma_1|\vec{n}_{\sigma_1} + |\sigma_2|\vec{n}_{\sigma_2})$$

We can express the flux of $K_T\nabla N_j$ on $\partial V_i \cap T$ using the outward normals at edges of the triangle T. To do so, we use the Gaussian theorem:

$$\int_{\partial V} \vec{n}d\sigma = 0 \quad (8)$$

where V is a surface with the boundary ∂V. We take V as a surface limited by Σ_1, Σ_2, σ_1 and σ_2. Then, we get:

$$a_{ij}^{flow}(T) = K_T\nabla N_j.(|\Sigma_1|\vec{n}_{\Sigma_1} + |\Sigma_2|\vec{n}_{\Sigma_1})$$

Taking into account that:

$$|\Sigma_1| = \frac{1}{2}|x_ix_j|\ |\Sigma_2| = \frac{1}{2}|x_ix_k|$$

and using (8), we get:

$$\begin{aligned} a_{ij}^{flow}(T) &= \frac{1}{2}K_T\nabla N_j.\left(|x_ix_j|\vec{n}_{\Sigma_1} + |x_ix_k|\vec{n}_{\Sigma_2}\right) \\ &= -\frac{1}{2}K_T\nabla N_j.\left(|x_jx_k|\vec{n}_{jk}\right) \end{aligned} \quad (9)$$

where $\vec{n}_{jk}$ is the outward unit normal at the edge (x_jx_k) of T. We recall that $\nabla N_j = -\frac{|x_ix_k|}{2|T|}\vec{n}_{\Sigma_2}$, then we get:

$$a_{ij}^{flow}(T) = \frac{|x_ix_k|}{2|T|}\frac{|x_jx_k|}{2|T|}\left(K_T\vec{n}_{\Sigma_2}.\vec{n}_{jk}\right)|T| \quad (10)$$

Finally, we incorporate the boundary conditions in (7) to obtain the linear system for the flow equation which is solved by the preconditioned conjugate gradient method. The preconditioning step utilizes incomplete Gaussian elimination.

Finally, the Darcy velocity $\vec{q}$, performed as a post-processing step, is approximated by a piecewise constant in each element T, denoted by $\vec{q}_T$, and given by:

$$\vec{q}_T = -\sum_{j\in T} P_j K_T \nabla N_j \tag{11}$$

For each vertex x_j of T, we have $\nabla N_j = -\frac{|x_i x_k|}{2|T|}\vec{n}_{\Sigma_2}$ and then we can express $\vec{q}_T$, using the opposite edge F_j of the vertex x_j in T and $\vec{n}_j$ the outward unit normal vector at F_j, as following:

$$\vec{q}_T = \frac{1}{2|T|}\sum_{j\in T} P_j |F_j| K_T \vec{n}_j \tag{12}$$

2.2 Discretization of the Transport Equation

Discretization of the concentration Equation (3) is performed by using a vertex-centred finite volume method, (*e.g.*, [2]), with a semi-implicit time stepping, the time discretization is implicit for the diffusion term and it is explicit for the convective term. The diffusion term is discretized by piecewise linear conforming finite elements, whereas the convective term is approximated with the aid of a Godunov scheme. Let us mention that a fully implicit scheme is also available in the code MELODIE.

Let C_i^n be an approximation of C at the point (x_i, t_n). First, we integrate Equation (3) over the control volume V_i, we apply the divergence theorem, a semi-implicit time discretization, the mass lumping in the accumulation term and a full upwind stabilization in the convective term, resulting in the following discrete concentration equation:

$$\omega_i |V_i| \frac{C_i^n - C_i^{n-1}}{\tau_n} - \int_{\partial V_i} \left(D\nabla C^n - \vec{q} C^{n-1}\right).\vec{n} d\sigma = |V_i| f_i^n \tag{13}$$

where $\omega_i = \frac{1}{|V_i|}\int_{V_i}\omega(x)dx$ and $f_i^n = \frac{1}{|V_i|}\int_{V_i} f(x,t_n)dx$

The discretization for the diffusive flux in (13) is performed using the same steps as above for the pressure equation. We have:

$$-\int_{\partial V_i} D\nabla C^n.\vec{n} d\sigma = \sum_{j\in V_T(\mathrm{i})} a_{ij}^{diff}(T)(C_j^n - C_i^n) \tag{14}$$

where:

$$a_{ij}^{diff}(T) = \frac{|x_i x_k|}{2|T|}\frac{|x_j x_k|}{2|T|} D_T \vec{n}_{\Sigma_2}.\vec{n}_{jk}|T| \tag{15}$$

with D_T is an approximation of the diffusion-dispersion tensor D in T.

To approximate the convective flux, we use the Godunov scheme. We have:

$$\int_{\partial V_i} C^{n-1}\vec{q}.\vec{n} d\sigma \approx \sum_{T;i\in T}\left(|\sigma_1| C_{|\sigma_1}^{n-1}\vec{q}_T.\vec{n}_{\sigma_1} + |\sigma_2| C_{|\sigma_2}^{n-1}\vec{q}_T.\vec{n}_{\sigma_2}\right. \tag{16}$$

On the dual edge σ_1 separating the vertices i and j, we approximate $C_{|\sigma_1}^{n-1}\vec{q}_T.\vec{n}_{\sigma_1}$ as following:

$$C_{|\sigma_1}^{n-1}\vec{q}_T.\vec{n}_{\sigma_1} \approx C_i^{n-1}(\vec{q}_T.\vec{n}_{\sigma_1})^+ + C_j^{n-1}(\vec{q}_T.\vec{n}_{\sigma_1})^- \tag{17}$$

where for $r \in \mathbf{R}$, $r^+ = \max\{0, r\}$ and $r^- = \min\{0, r\}$. Note that $C_{|\sigma_1}^{n-1}$ is approximated taking care of the flow direction. Denote by:

$$\begin{aligned} a_{ij}^{conv}(T) &= |\sigma_1|(\vec{q}_T.\vec{n}_{\sigma_1})^-,\ a_{ii}^{conv}(T) \\ &= |\sigma_1|(\vec{q}_T.\vec{n}_{\sigma_1})^+ + |\sigma_2|(\vec{q}_T.\vec{n}_{\sigma_2})^+ \end{aligned} \tag{18}$$

the elementary convective terms. Then (17) implies:

$$\begin{aligned} &\int_{\partial V_i} C^{n-1}\vec{q}.\vec{n} d\sigma \approx \sum_{T;i\in T} a_{ii}^{conv}(T)C_i^{n-1} + a_{ij}^{conv}(T)C_j^{n-1} \\ &+ a_{ik}^{conv}(T)C_k^{n-1} = \sum_{T;i\in T}\{a_{ii}^{conv}(T)C_i^{n-1} + \sum_{j\in V_T(i)} a_{ij}^{conv}(T)C_j^{n-1}\} \end{aligned} \tag{19}$$

Finally, the scheme could be written in the following form:

$$\begin{aligned} &\omega_i|V_i|C_i^n + \tau_n \sum_{T;i\in T}\sum_{j\in V_T(\mathrm{i})} a_{ij}^{diff}(T)\left(C_j^n - C_i^n\right) \\ &= \left[\omega_i|V_i| - \tau_n \sum_{T;i\in T} a_{ii}^{conv}(T)\right] C_i^{n-1} \\ &-\tau_n \sum_{T;i\in T}\sum_{j\in V_T(\mathrm{i})} a_{ij}^{conv}(T)C_j^{n-1} - \tau_n|V_i|f_i^n \end{aligned} \tag{20}$$

Then, we incorporate the boundary conditions to obtain, at each time step, the linear system which is solved by the preconditioned conjugate gradient method. The preconditioning step utilizes incomplete Gaussian elimination.

Let us end this section by the following remark.

Remark 1. *To ensure the discret maximum principle and hence the stability of this scheme we define locally the CFL condition as*:

$$\left(\frac{\omega_i|V_i|}{\tau_n} - \sum_{T;i\in T} a_{ii}^{conv}(T)\right) \geq 0 \tag{21}$$

Taking into account (18), we get the following estimation for a_{ii}^{conv}:

$$a_{ii}^{conv} \leq |\partial V_i \cap T||\vec{q}_T.\vec{n}|_{\max} \tag{22}$$

where $|\vec{q}_T.\vec{n}|_{\max}$ *is the maximum of* $|\vec{q}_T.\vec{n}|$ *over all dual edges belonging to* T.

Furthermore we get:

$$\omega_i|V_i| = \sum_{T;i\in T} |V_i \cap T|\omega_i \tag{23}$$

It follows thanks to (22) and (23) that (21) holds true if:

$$\tau \leq \frac{\omega_i|V_i \cap T|}{|\partial V_i \cap T||\vec{q}_T.\vec{n}|_{\max}}$$

Then we define the following CFL condition:

$$CFL = \frac{\min\{\omega_i|V_i \cap T|;\ i \in T\}}{\max\{|\partial V_i \cap T|;\ i \in T\}\max\{|\vec{q}_T.\vec{n}|_{\max};\ i \in T\}} \tag{24}$$

3 *A POSTERIORI* ESTIMATORS AND ADAPTIVE ALGORITHMS

In this section, we derive an adaptive numerical technique using the finite volume approximation described in the previous section. The proposed error estimators were suggested in [8] for vertex-centered finite volumes method. Here, we extend this strategy to finite volumes finite elements discretization and for more complex geometry. The estimator was obtained by dual volumes summation of the residuals, while in the current work it is obtained by summation over the underlying triangulation. The method expresses the error in terms of the residual of the approximate solution. Based on the error estimators, the mesh adaptivity relies on mesh generator. A new mesh must be generated at each time step. After that, there are two alternatives: either restart the computation from scratch or project all the information from the old mesh to the new mesh. The two meshes may have very different topologies and number of elements and the number of degrees of freedom can change arbitrarily to meet a prescribed accuracy. The initial mesh does not drastically influence the adaptive process, because a new mesh is rebuilt at each step.

Each triangulation $\mathscr{T}_h^{n+1}$ is derived from $\mathscr{T}_h^n$ by refining some elements of $\mathscr{T}_h^n$ into a few sub-elements or by derefining some elements into a new elements. We denote $D^n = D(t_n)$, $\vec{q}^n = \vec{q}(t_n)$ and $f^n = f(t_n)$, and we introduce D_h^n (resp. f_h^n) a piecewise approximation of D^n (resp. f^n). In the following, C_h^n will denote the finite volume approximation of C^n, such that $C_h^n = \sum_{i=1}^N C_i^n N_i$, and $\vec{q}_h^n$ the piecewise P_0 approximation of $\vec{q}^n$ expressed by the hydraulic head.

Following [30] and [8], we define the residuals and inter-element jumps of the approximation:

$$R_{h|T}^n = \left(f_h^n - \omega_T \frac{C_h^n - C_h^{n-1}}{\tau_n} + div\left(D_h^n \nabla C_h^n\right) - div\left(\vec{q}_h^{n-1} C_h^{n-1}\right)\right) \tag{25}$$

where T stands for the current element $T \in \mathscr{T}_h^n$. Let:

$$r_{h|E}^n = \left[D_h^n \nabla C_h^n.\vec{n}_E\right] \tag{26}$$

where $[,]_E$ denotes the difference between limits from either side of the edge $E \in \mathscr{E}_h^n$, and $\vec{n}_E$ is the outward unit normal vector at the edge E. Let:

$$z_{h|\gamma}^n = \vec{q}_h^{n-1}.\vec{n}_\gamma\left(C_h^{n-1}(x_i) - C_h^{n-1}(x_j)\right) \tag{27}$$

where $\gamma \in \Gamma_h^n$ is an edge of the dual decomposition $\mathscr{V}_h^n$ and $\vec{n}_\gamma$ is the outward unit normal vector at γ.

We define local spatial error indicators:

$$(\eta_R^n)^2 = \sum_{T\in\mathscr{T}_h^n} h_T^2 ||R_h^n||_{0,T}^2 \tag{28}$$

diffusive jumps:

$$(\eta_r^n)^2 = \sum_{E\in\mathscr{E}_h^n} h_E ||r_h^n||_{0,E}^2 \tag{29}$$

and convective jumps:

$$(\eta_z^n)^2 = \sum_{\gamma\in\Gamma_h^n} h_\gamma ||z_h^n||_{0,\gamma}^2 \tag{30}$$

where $||v||_{0,S} = \int_S v^2 dx$ denotes the L^2 norm for any function v and any subset S of Ω.

The global spatial error indicator is given by:

$$(\eta_{sp}^n)^2 = (\eta_R^n)^2 + (\eta_r^n)^2 + (\eta_z^n)^2 \tag{31}$$

For each $n \in \{1, ..., N\}$, we define the temporal error indicator as:

$$\eta_{tm}^n = \left(\frac{\tau_n}{3}(||D_h^n)^{\frac{1}{2}}\nabla(C_h^n - C_h^{n-1})||_{0,\Omega}^2 + ||div(\vec{q}_h^{n-1}(C_h^{n-1} - C_h^n))||_{0,\Omega}^2\right)^{\frac{1}{2}} \quad (32)$$

With the family $(C_h^n)_{0\le n\le N}$, we associate the function $C_{h\tau}$ in $[0,T]$ which is linear on each interval $[t_{n-1}, t_n]$, $1 \le n \le N$, and equal to C_h^n at t_n, $0 \le n \le N$. This function writes, for $1 \le n \le N$:

$$C_{h\tau} = C_h^{n-1} + \frac{t - t_{n-1}}{\tau_n}\left(C_h^n - C_h^{n-1}\right)$$

We define the norm $||C_{h,\tau}||_{(t_{n-1},t_n)}$ as follows:

$$||C_{h,\tau}||_{(t_{n-1},t_n)}^2 = \int_{t_{n-1}}^{t_n} (||(D_h^n)^{\frac{1}{2}}C_{h,\tau}||_{0,\Omega}^2 + ||(div\vec{q}_h^n)C_{h,\tau}||_{0,\Omega}^2)$$

We define the global error indicator as follows:

$$\overline{\eta} = \sum_{n=1}^{N}(\eta_{sp}^n + \eta_{tm}^n)^2$$

Then for an approximate solution $C_{h,\tau}$, we define the relative error estimator η_r by:

$$\eta_r = \frac{\overline{\eta}}{\sum_{n=1}^{N}||C_{h,\tau}||_{(t_{n-1},t_n)}}$$

Our aim is to control the relative error between the exact and approximated solution by a prescribed tolerance. In the following, we give an overview of the basis time-stepping routine and then describe in detail each time step of the algorithm. We denote by $\mathcal{N}_{\mathcal{T}_h^{n-1}}$ the number of triangles belonging to $\mathcal{T}_h^{n-1}$.

We present here an adaptive algorithm based on the above *a posteriori* error estimates which is designed to ensure that the relative energy error between the exact and approximate solutions will be below a prescribed tolerance. The spatial refinement-derefinement is performed using the maximum strategy, while the temporal adaption is based on the temporal error indicator and the CFL condition. Let ε a predefined parameter. The aim is to build an adaptive mesh $\mathcal{T}_h^n$, $n = 1, ..., N$ for an adapted time step τ_n such that the error indicators ensure that the relative error estimator is below the prescribed parameter ε, such that $\eta_r \le \varepsilon^2$ so as to equilibrate the space and the time estimators.

For a given time level t_{n-1}, we set:

$$\mathcal{T}ol = \varepsilon\frac{||u_{h\tau}||_{(t_{n-1},t_n)}}{\sqrt{2}}$$

We denote by $0 < \delta_{ref} < 1$ and $0 < \delta_{deref} < 1$ two parameters. For practical implementation purposes and because computer limitations, we introduce maximal level parameters $\mathcal{N}_{sp}$, $\mathcal{F}r_{sp}$ and $\mathcal{F}r_{tm}$, where:

- $\mathcal{N}_{sp}$, is the limit number (level) of refinement,
- $\mathcal{F}r_{sp}$, the frequence of using the spatial refinement-derefinement process,
- $\mathcal{F}r_{tm}$, the frequence of using the temporal adaptation process,
- $\mathcal{C}fl_{lim}$, a prescribed value constraint that the CFL condition limit does not exceed.

Adaptive algorithm

Let an initial mesh $\mathcal{T}_h^0$ *, and an initial time step* τ_0
Set $n = 1$ *and* $t^1 = t^0 + \tau^0$
Time iterations: **While** $t^n \le T$
DO
Resolve $C_h^n = Sol(C_h^{n-1}, \tau^{n-1}, \mathcal{T}_h^{n-1})$
Estimmate η_{sp}^n *and* η_{tm}^n
Refine elements $T \in \mathcal{T}_h^{n-1}$ *where* $\eta_{sp|T}^n \ge \delta_{ref}$ *max* $\{\eta_{sp|K}^n, / K \in \mathcal{T}_h^{itn-1}\}$, *or*
Derefine elements $T \in \mathcal{T}_h^{n-1}$ *such that* $\eta_{sp|T}^n \le \delta_{deref}$ $\sum_{K\in}\mathcal{T}_h^{n-1}\eta_{sp|K}^n/\mathcal{N}_{\mathcal{T}_h^{n-1}}$ *to obtain the final mesh* $\mathcal{T}_h^n$ *such that the refinement'slevel is less than* $\mathcal{N}_{sp}$
While $\eta_{sp}^n \ge \mathcal{T}ol$
Depending on the value fr_{tm}
If $\eta_{tm}^n > \mathcal{T}ol$ *and* $CFL < \mathcal{C}fl_{lim}$
Set $t^n = t^n - \tau^{n-1}$ *and* $\tau^{n-1} = \tau^{n-1}/2$
Else
Set $t^n = t^n + \tau^{n-1}$ *and* $\tau^{n-1} = 1.1\tau^{n-1}$
Save the approximation C_h^n, *the mesh* $\mathcal{T}_h^n$ *and the temporal step size* τ^n.
Set $n = n + 1$.

The mesh refinement algorithm is based on bisecting an element into three triangles. Suppose that a set of elements are scheduled for refinement, then those elements are bisected by creating a gravity center node, see Figure 2. The derefinement process consists in deleting every couple of triangles, based on error indication information. If so the mesh would be coarsened to the one shown in Figure 3 or Figure 4. Suppose that error indicators reveal that these elements may be coarsened. The strategy of collapsing the vertices of the current triangle onto his gravity center is done by deleting all edges connected to those vertices. After coarsening or refining we update the mesh calling a Delaunay correction program to ensure that the mesh respects the empty circle criterion (*Fig. 5, 6*).

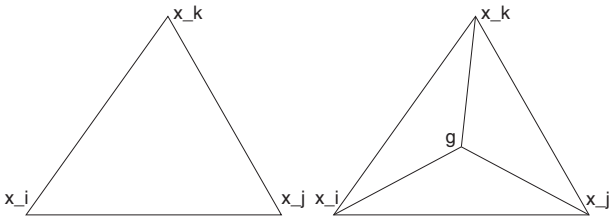

Figure 2

Refinement process of the current triangle.

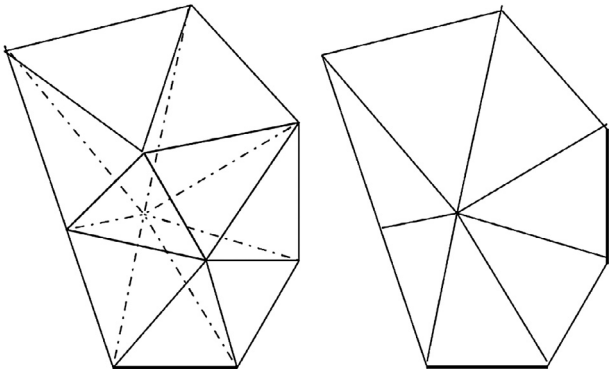

Figure 4

Derefinement of the boundary elements.

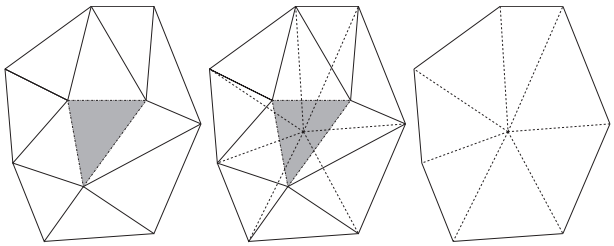

Figure 3

Coarsening of a polygonal region.

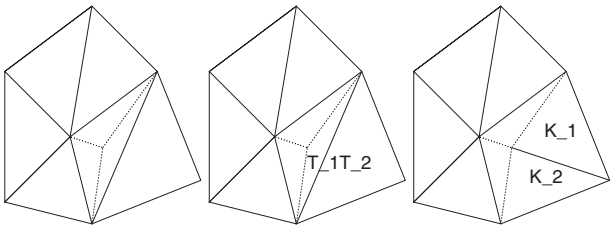

Figure 5

Refinement process.

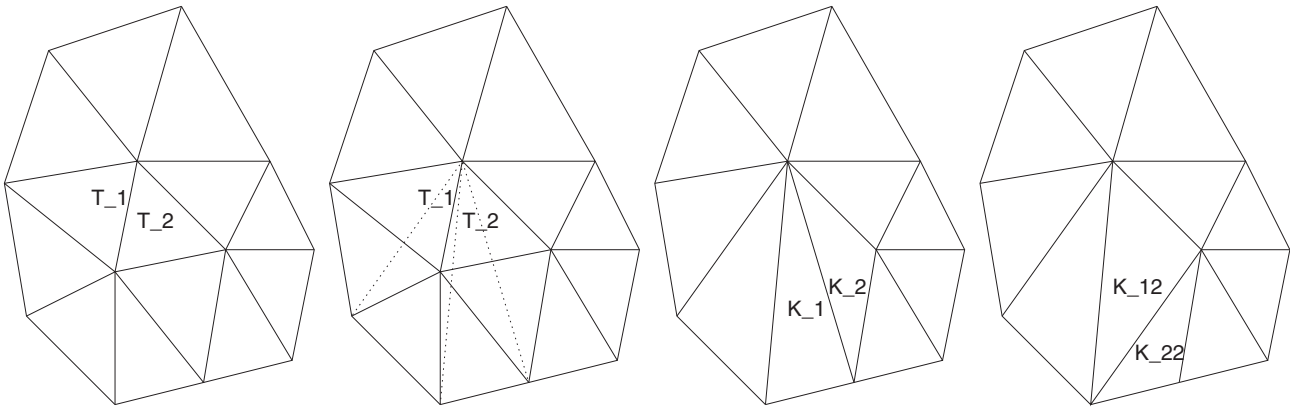

Figure 6

Derefinement process.

The shape of elements containing small or large angles that were created during refinement or coarsening may be improved by edge swapping. This procedure operates on pairs of triangles T_1 and T_2, which violate the empty circle criterion, that share a common edge E. The edge swapping occurs deleting this edge and the empty circle criterion is satisfied for the triangles K_1 and K_2 Figure 7. The process is continued until all irregular triangles are removed. As such, swapping will have to provide mesh quality.

Remark 2. *In addition of the set of elements that are marked in this way, we also mark all their neighbors with a common edge. We moreover add to this set those elements that now have more than half of the neighbors marked (Fig. 3).*

Remark 3. *In order to approximate the flux at the fine grid in the boundaries we introduce additional (auxiliary) points, in which the solution is obtained by interpolation on the coarse grid (Fig. 8).*

We end up this section by the following remark about the interpolation of the solution after a modification of the mesh.

Remark 4. *Note that the solution interpolation is also a key point in the mesh adaptation algorithm. For that, we need an interpolation scheme to transfer the information of the solution from the current mesh to the newly adapted mesh. Before proceeding to mesh adaption, we save the history of the current mesh. The new generated vertices are located in the current mesh by identifying the elements containing them. Then an interpolation scheme is used to extract the information from the solution. More precisely, the mesh refinement algorithm is based on bisecting an element into three triangles by adding a gravity center node. Then we assign to this new node the average of the values of the solution to the vertices of the triangle containing it. The temporal error indicators are used to control the errors due to the solution interpolation stage. The software automatically selects time steps to satisfy a prescribed (local) temporal error tolerance and to maintain stability.*

4 NUMERICAL RESULTS

In this section, we illustrate the adaptive methodology. We study the performance of the algorithm by looking at the spatial adaptation of the mesh and aim at obtaining a good distribution of nodes, in taking into account also the temporal adaption. The following numerical two examples are performed to demonstrate the implementation of the proposed algorithm. In the first example, we verify our underlying adaptive numerical algorithm. In the second one, we present a numerical example for a waste-disposal in a complex domain.

4.1 Example 1: Heterogeneous Domain with One Source

This scenario consists of a pulse of activity in a heterogeneous domain. This example helps to get the first conclusions about the efficiency of the adaptive method. We consider the domain $\Omega =]0, 50[\times]0, 20[$ composed of two parts, *i.e.*, the left medium $\Omega_l =]0, 20[\times]0, 20[$ and the right medium $\Omega_r =]20, 50[\times]0, 20[$ (*Fig. 9*). The values of physical parameters are presented in Table 1. The dispersivity is isotropic for the right medium and anisotropic for the left. The flow calculation is carried out with a condition of constant pressure head on the right vertical limit of a value of 30 meters and on the left vertical limit of a value of 0 meter. The initial concentration is 10^4 Bq at the center of the left medium and releases immediately at the first step of time of the simulation. The transport equation is solved for a short time interval (0-5 years) with adapted time step size.

For this domain, the adaptive strategy is applied. The error indicators are computed for each element T at time

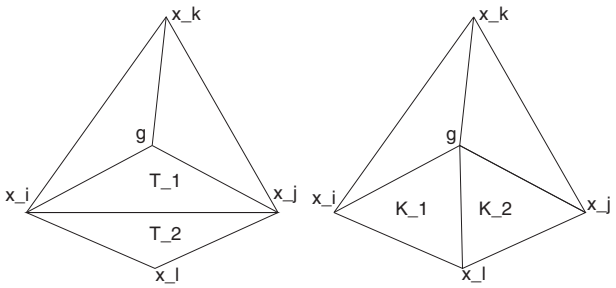

Figure 7
The edge swap mesh modification.

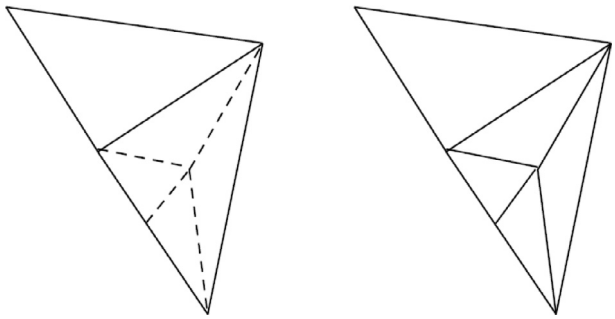

Figure 8
Refinement of the boundary elements.

TABLE 1
Physical parameters of the two medias

Medium	K (m.year^{-1})	ω	α_l (m)	α_t (m)	d_e (m^2.year^{-1})
Ω_l	1.0	0.1	1.0	5e-05	0.0
Ω_r	1.0	0.01	0.5	0.5	0.0

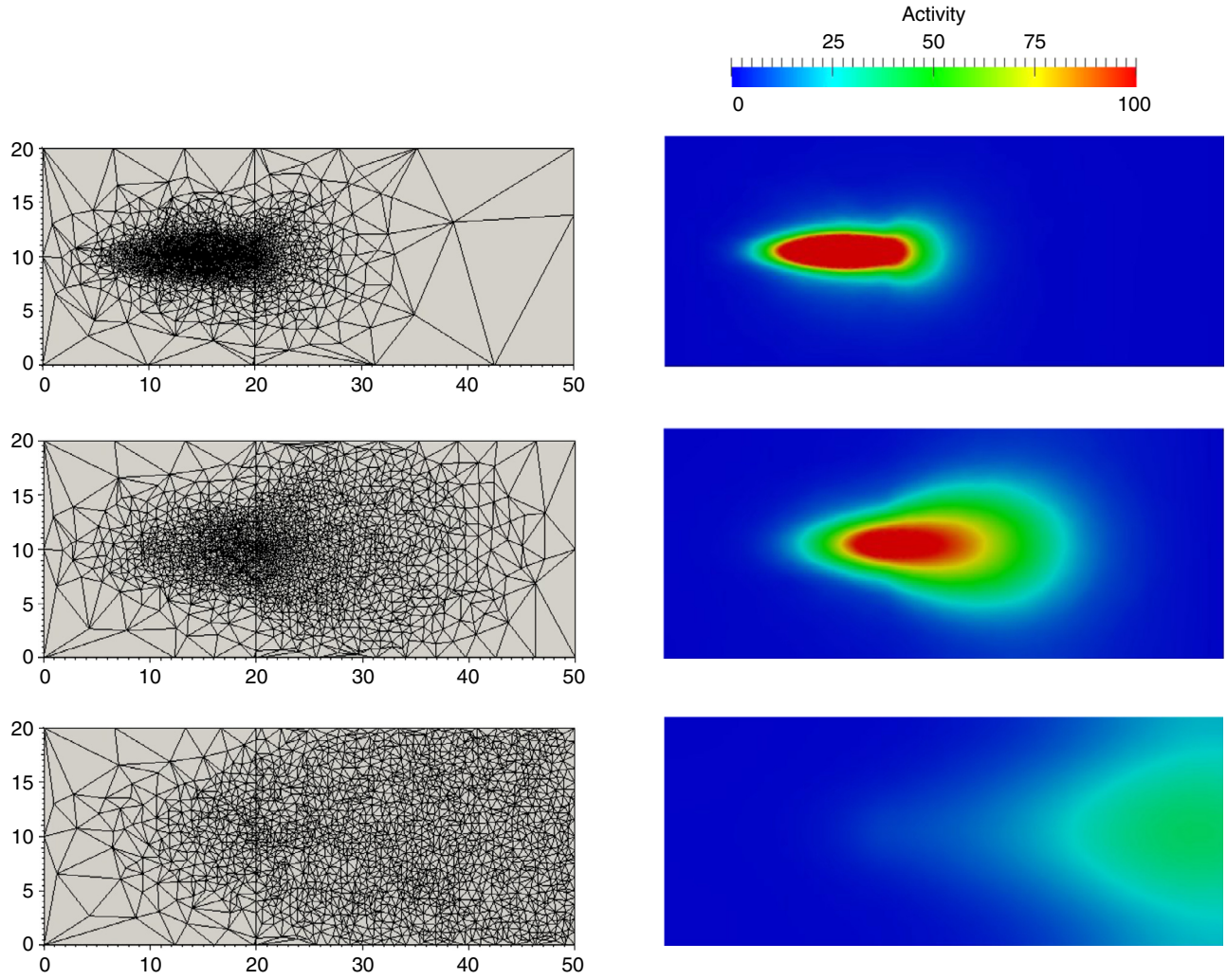

Figure 9

Adaptive mesh (left) and concentration (right) after 1, 2 and 5 years.

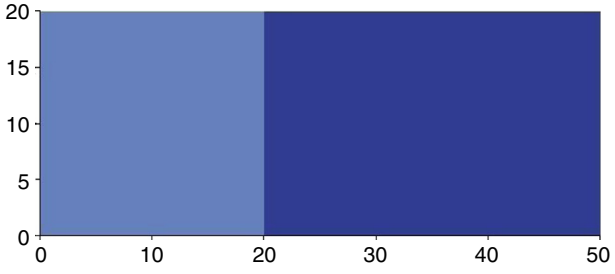

Figure 10

Heterogeneous domain: Ω_l (left) and Ω_r (right).

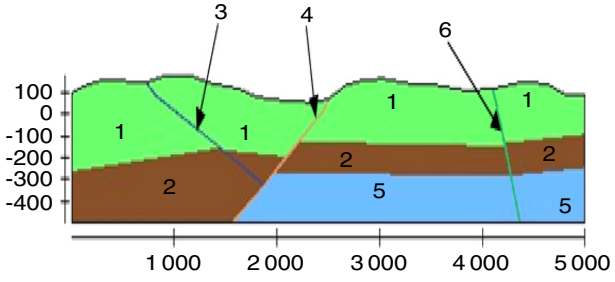

Figure 11

A heterogeneous porous medium of a realistic model.

t_n: then elements with the largest error indicator values are refined, and other elements with the smallest error indicator values are coarsened. The propagation of the mesh and the corresponding activities till the end time is displayed in Figure 10. The simulation results show that the contaminant moves from the left in a narrow

TABLE 2
Physical parameters of the media

Medium	K (m.year^{-1})	ω	α_l (m)	α_t (m)	d_e (m^2.year^{-1})
1	10.0	0.15	0.5	0.5	0.05
2	0.0001	0.3	1.0	1.0	0.01
3	500.0	0.2	12.0	6.0	0.5
4	0.05	0.2	5.0	0.5	1.0
5	50.0	0.17	10.0	1.0	0.05
6	5.0	0.15	8.0	0.4	2.0

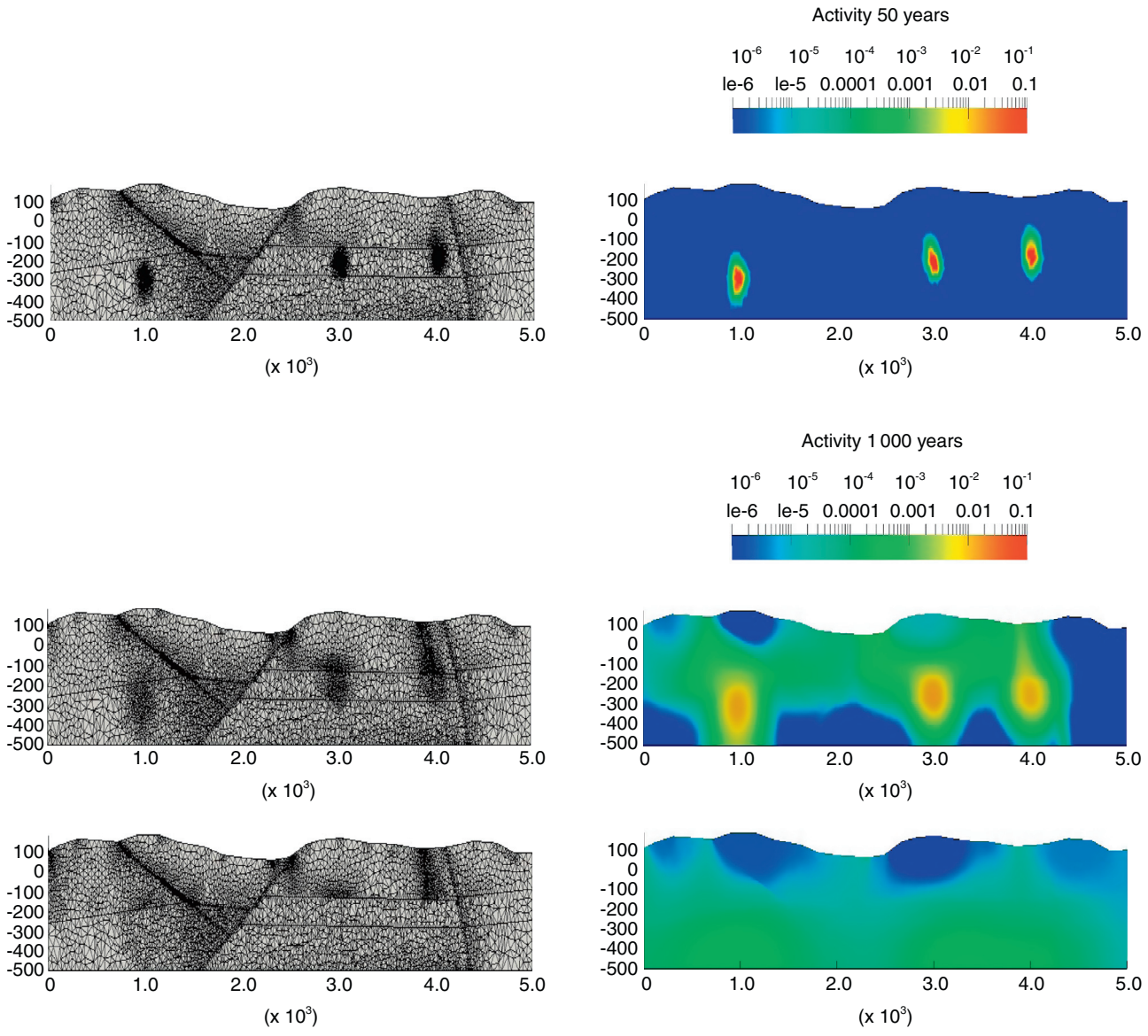

Figure 12

Adaptive mesh (left) and concentration (right) after 50, 1000 and 10 000 years.

plume and wide in the right medium after the interface between the two media. The mesh follows the movement of the plume. This numerical test shows that the proposed adaptive strategy is effective for guiding mesh adaption.

4.2 Example 2: Waste-Case Model with Different Sources

One of goals of this work is to simulate the flow of water and transport for 10 000 years in realistic conditions. The model is a cross cutting geological of 5 000 meters long and 600 meters high with 3 different layers cutting by 3 faults cf. Figure 11. The different values of parameters are presented in Table 2. The groundwater flow is under steady state condition. The flow calculation is carried out with a condition of the pressure head equal to the topographic level on the top of the model by applying a first spatial adaptation of the a posteriori error method. On the field of hydraulic head obtained, the simulation of the immediate release of the three sources of waste is modeled with a condition that the adapt mesh cannot be less precise than the first mesh on which the water flow calculation is made. The simulation time is 10 000 years and the calculation of the transport of the contaminant is made upon all the domains. Figure 12 displays the state of the concentration in the cross cutting for 3 dates of the simulation and the corresponding propagation of the mesh like for the example 1. In this case, the adaptive strategy also performs fairly well with mesh refinement which is made almost solely around sources points.

CONCLUSION

In this paper, we presented an adaptive mesh refinement algorithm for single phase flow in porous media. The processes modeled are miscible flow of an incompressible fluid with a dissolved radioactive solute to simulate the evolution of radionuclide migration in a nuclear waste repository. The resulting system is discretized by a vertex-centred finite volume method. The method was implemented in the software MELODIE. This leads to a considerable improvement in computational efficiency. The adaptive strategy has been illustrated by means of numerical examples in an academic scenario and a realistic scenario. The above results illustrate that the proposed adaptive mesh refinement is capable of tackling in a robust and accurate fashion various physical phenomena relevant to flow and transport of radionuclides in heterogeneous porous media. Our goal in future work will be to extend this approach to more realistic 3D problems.

ACKNOWLEDGMENTS

This work was partially supported by the IRSN (PRP-DGE/SEDRAN/BERIS) Fontenay-Aux-Roses, France, whose support is gratefully acknowledged.

REFERENCES

1 OECD/NEA (2006) Safety of geological disposal of high-level and long-lived radioactive waste in France, An International Peer Review of the "Dossier 2005 Argile" Concerning Disposal in the Callovo-Oxfordian Formation. OECD Publishing. Available online at: https://www.oecd-nea.org/rwm/reports/2006/nea6178-argile.pdf.

2 Amaziane B., El Ossmani M., Serres C. (2008) Numerical modeling of the flow and transport of radionuclides in heterogeneous porous media, *Comput. Geosci.* **12**, 4, 83-98.

3 Bourgeat A., Kern M., Schumacher S., Talandier J. (2004) The couplex test cases: Nuclear waste disposal simulation, *Comput. Geosci.* **8**, 2, 437-449.

4 Chavent G., Jaffré J. (1986) *Mathematical Models and Finite Elements for Reservoir Simulation*, Elsevier North–Holland, Amsterdam.

5 Chen Z., Huan G., Ma Y. (2006) *Computational Methods for Multiphase Flows in Porous Media*, SIAM, Philadelphia.

6 Helmig R. (1997) *Multiphase Flow and Transport Processes in the Subsurface*, Springer, Berlin.

7 Achdou Y., Bernardi C., Coquel F. (2003) *A priori* and *a posteriori* analysis of finite volume discretizations of Darcy's equations, *Numer. Math.* **96**, 1, 17-42.

8 Amaziane B., Bergam A., El Ossmani M., Mghazli Z. (2009) *A posteriori* estimators for vertex centred finite volume discretization of a convection-diffusion-reaction equation arising in flow in porous media, *Int. J. Numer. Methods Fluids* **59**, 3, 259-284.

9 Angermann L. (1995) Balanced *a posteriori* error estimates for finite volume type discretization of convection-dominated elliptic problems, *Computing* **55**, 305-323.

10 Bergam B., Mghazli Z., Verfürth R. (2003) *A posteriori* estimates for a finite-volume scheme for a nonlinear problem, *Numer. Math.* **95**, 599-624.

11 Bürkle D., Ohlberger M. (2002) Adaptive finite volume methods for displacement problems in porous media, *Comput. Vis. Sci.* **5**, 2, 95-106.

12 Cancès C., Pop I.S., Vohralik M. (2013) An *a posteriori* error estimate for vertex-centered finite volume discretizations of immiscible incompressible two-phase flow, *Math. Comp.* (to appear).

13 Carstensen C., Lazarov R., Tomov S. (2005) Explicit and averaging *a posteriori* error estimates for adaptive finite volume methods, SIAM, *Numer. Anal.* **42**, 6, 2496-2521.

14 Ern A., Vohralik M. (2011) A unified framework for *a posteriori* error estimation in elliptic and parabolic problems with application to finite volumes, Finite volumes for complex applications. VI. Problems & perspectives. Volume 1, 2, 821837, *Springer Proc. Math., 4*, Springer, Heidelberg.

15 Ju L., Wu W., Zhao W. (2009) Adaptive finite volume methods for steady convection-diffusion equations with mesh optimization, *Discrete Contin. Dyn. Syst. Ser. B.* **11**, 3, 669-690.

16 Lazarov R., Tomov S. (2002) *A posteriori* error estimates for finite volume element approximations of convection-diffusion-reaction equations, *Comput. Geosci.* **6**, 483-503.

17 Nicaise S. (2006) *A posteriori* error estimates for some cell centered finite volume methods for diffusion-convection–reaction problems, SIAM, *Numer. Anal.* **44**, 949-978.

18 Ohlberger M. (2001) *A posteriori* error estimates for vertex centered finite volume approximations to singularly perturbed nonlinear for convection-diffusion-reraction equations, *Numer. Math.* **87**, 737-761.

19 Ohlberger M. (2001) *A posteriori* error estimates for vertex centred finite volume approximations of convection-diffusion-reaction equation, M2AN, *Math. Model. Numer. Anal.* **35**, 355-387.

20 Ohlberger M. (2009) A review of *a posteriori* error control and adaptivity for approximations of non-linear conservation laws, *Int. J. Numer. Methods Fluids* **59**, 3, 333-354.

21 Ohlberger M., Rohde C. (2002) Adaptive finite volume approximations for weakly coupled convection dominated parabolic systems, *IMA J. Numer. Anal.* **22**, 2, 253-280.

22 Pau G.S.H., Almgren A.S., Bell L.B., Lijewski M.J. (2009) A parallel second-order adaptive mesh algorithm for incompressible flow in porous media, *Philos. Trans. R. Soc. Lond. Ser. A Math. Phys. Eng. Sci.* **367**, 1907, 4633-4654.

23 Pau G.S.H., Bell J.B., Almgren A.S., Fagnan K.M., Lijewski M.J. (2012) An adaptive mesh refinement algorithm for compressible two-phase flow in porous media, *Comput. Geosci.* **16**, 577-592.

24 Vohralik M. (2008) Residual flux-based *a posteriori* error estimates for finite volume and related locally conservative methods, *Numer. Math.* **111**, 1, 121-158.

25 Vohralik M. (2011) *A posteriori* error estimates for combined finite volume–finite element discretizations of reactive transport equations on nonmatching grids, *Comput. Methods Appl. Mech. Eng.* **200**, 597-613.

26 Melodie software, http://www.irsn.fr/EN/Research/Scientific-tools/Computer-codes/Pages/MELODIE-software-3133.aspx.

27 Mathieu G., Dymitrowska M., Bourgeois M. (2008) Modeling of radionuclide transport through repository components using finite volume finite element and multidomain methods, *Phys. Chem. Earth* **33**, S216-S224.

28 Bastian P. (1999) *Numerical computation of multiphase flow in porous media*, Habilitationsschrift.

29 Afif M., Amaziane B. (2008) *Numerical simulation for the anisotropic benchmark by a vertex-centred finite volume method, Finite Volumes for Complex Applications V*, 693-704, ISTE, London.

30 Verfürth R. (2005) Robust *a posteriori* error estimates for nonstationary convection–diffusion equations, SIAM, *J. Numer. Anal.* **43**, 1783-1802.

Manuscript accepted in July 2013
Published online in December 2013